On the reliability of reverse engineering results

Tatiana V. Amotchkina,[1,5,*] Michael K. Trubetskov,[1,2] Vladimir Pervak,[3] Boris Romanov,[4] and Alexander V. Tikhonravov[1]

[1]Research Computing Center, Moscow State University, Leninskie Gory, 119991, Moscow, Russia

[2]Max Planck Institute of Quantum Optics, Hans-Kopfermann-Str. 1, 85748 Garching, Germany

[3]Ludwig-Maximilians-Universität München, Am Coulombwall 1, 85748 Garching, Germany

[4]Leybold Optics GmbH, Siemensstrasse 88, 63755 Alzenau, Germany

[5]QUEST. Centre for Quantum Engineering and Space-Time Research, Welfengarten 1, 30167 Hannover, Germany

*Corresponding author: tatiana@srcc.msu.ru

Received 3 May 2012; revised 27 June 2012; accepted 27 June 2012;
posted 28 June 2012 (Doc. ID 167892); published 30 July 2012

Determination of actual parameters of manufactured optical coatings (reverse engineering of optical coatings) provides feedback to the design-production chain and thus plays an important role in raising the quality of optical coatings production. In this paper, the reliability of reverse engineering results obtained using different types of experimental data is investigated. Considered experimental data include offline normal incidence transmittance data, offline ellipsometric data, and online transmittance monitoring data recorded during depositions of all coating layers. Experimental data are obtained for special test quarter-wave mirrors with intentional errors in some layers. These mirrors were produced by a well-calibrated magnetron-sputtering process. The intentional errors are several times higher than estimated errors of layer thickness monitoring, and the reliability of their detection is used as a measure of reliability of reverse engineering results. It is demonstrated that the most reliable results are provided by online transmittance data.

OCIS codes: 310.6805, 310.3840, 310.1620, 310.1860, 310.6860.

1. Introduction

Reliable determination of actual optical parameters of layers of deposited multilayer coatings (so-called reverse engineering of optical coatings [1,2]) plays a key role in advancing the quality of optical coatings production. Reverse engineering results provide feedback to the design-production chain because they can be used for adjusting deposition parameters, recalibrating monitoring systems, and improving control of thicknesses of individual layers [1,3]. These results may also be useful in the course of establishing adequate levels of simulation parameters in cases when computational manufacturing is incorporated into the design-production chain [4].

From a mathematical point of view, reverse engineering is a typical ill-posed inverse problem, and specific numerical algorithms are required to solve this problem [5]. The complexity of this problem is connected with the ambiguity and instability of the problem solution [6–8].

One of the most popular approaches to reverse engineering is based on the postproduction analysis of normal incidence or quasi-normal incidence transmittance (T) and/or reflectance (R) data related to a produced coating sample. This approach is simple from an experimental point of view. Normal incidence transmittance and quasi-normal incidence reflectance can be measured with a sufficient accuracy using any UV-visible–near-IR dispersive or Fourier-transform spectrophotometer. However, this approach is quite complicated from a mathematical point of view because many unknown parameters are found from a

1559-128X/12/225543-09$15.00/0

single R or/and T data array. In order to determine layer parameters reliably, one should apply a sequence of physically meaningful models of optical constants and thickness errors [8]. There are situations when it is not possible in principle to find layer parameters from single R or/and T data arrays. As an example of such a situation, the reverse engineering of dispersive mirrors working in broadband spectral ranges can be considered. In this case, reflectance data are not informative, and other spectral characteristics (group delay or group delay dispersion) should be measured [8].

Another approach to reverse engineering is based on the analysis of multiangle R and T measurements taken for a produced multilayer coating [9]. In [9] we demonstrated that simultaneous analysis of reflectance and transmittance data taken at different angles of incidence (AOI) and for different polarization states increased the reliability of reverse engineering results.

Spectral ellipsometric data are used mainly for optical characterization of single thin films [10,11]. Numerical algorithms for reverse engineering of multilayer optical coatings on the basis of spectral ellipsometry are provided by several commercial software packages (see, for example, [10,12]). It is known that in some cases, ellipsometric data significantly reduce ambiguity and provide unique solutions to reverse engineering problems. In [13], ellipsometric data were used for characterization of digitized rugate coatings with the help of a general regularization approach [5]. In [14] it was proved that three layer structures "dielectric film–ultrathin metal-dielectric composite film–dielectric film" can be reliably characterized on the basis of ellipsometric data. Authors of [6] used ellipsometric measurements in combination with photometric measurements to reduce instability in the course of reverse engineering of hybrid antireflection coatings.

In recent years, reverse engineering algorithms based on multiscan measurements have been elaborated [4,15–17]. These multiscan measurements are typically transmittance or reflectance data recorded *in-situ* during the deposition process. Such multiscan data sets can be provided by broadband monitoring (BBM) systems [2,3,18]. Using multiscan data allows one to involve more input information in solving reverse engineering problems and to reduce the ambiguity of its solution.

In this paper, we investigated the reliability of reverse engineering results obtained on the basis of analysis of different experimental data sets. At the current state of art, this question has not been studied systematically. The primary goal of our paper was to reveal measurement data sets that are sufficient for providing reliable reverse engineering results. Our secondary goal was to demonstrate examples of data sets that may give wrong reverse engineering results.

As experimental basis, we produced samples of single layers and multilayer stacks. These stacks were quarter-wave mirrors (QWM) with intentionally imposed errors on thicknesses of several layers. We knew these errors with a high accuracy because the mirrors were produced using well-calibrated time monitoring control [19]. In our disposal we had several sets of measurement data, namely, multiscan transmittance measurements recorded in the course of the deposition process, quasi-normal R and T data related to produced samples, and ellipsometric data taken for the samples. We used two reverse engineering software tools in our research. These tools were OptiRE module of OptiLayer software ver. 8.85 [12] and Woollam WVASE32 ver. 3.770 [10].

In Section 2, we describe in detail our experimental samples and measurement data. In Section 3, we obtain reverse engineering results on the basis of analysis of different sets of measurement data and find that data sets provide reliable results. Our final conclusions are presented in Section 4.

2. Experimental Samples and Measurement Data

For our study, we produced six experimental samples. Two samples were the samples of single Ta_2O_5 and Si_2O_2 films on Suprasil substrates of 6.35 mm thickness. Geometrical thicknesses of the films were about 290 and 400 nm, respectively. We used these samples to verify consistency of characterization results obtained from different measurement data sets.

Four samples were the *test samples* of 15 layer QWM with a central wavelength of 600 nm. We used tantalum pentoxide as a high index material (odd layers) and silicon dioxide as a low index material (even layers). In the course of the deposition of test samples, intentional errors were imposed on thicknesses of several layers. We used these samples to check the reliability of reverse engineering results obtained on the basis of analysis of different measurement data sets.

The experimental samples were produced with magnetron-sputtering plant (HELIOS, Leybold Optics GmbH). This plant was equipped with two proprietary TwinMags magnetrons and a plasma source for plasma/ion assisting. The system was pumped by turbo-molecular pumps to $1 \cdot 10^{-6}$ m bar before the sputtering. Argon and oxygen were used for both magnetrons. The cathode power for Si (purity 99.999%) and Ta (purity 99.8%) targets were 4500 and 2500 W, respectively. The power applied to the Ta cathode was not constant because it operated in the oxygen control mode that guaranteed stable film properties. The gas pressure was $1 \cdot 10^{-3}$ m bar during the sputtering process. Oxygen was fed near the targets to oxidize the sputtering films. The distance from targets to the substrates was 100 mm. The deposition rates were approximately 0.5 nm/s for both materials.

In total, we performed four deposition runs. In the first and second deposition runs, we produced samples of single Ta_2O_5 and SiO_2 films.

In the third deposition run, we deposited two of the test samples simultaneously. Our turntable had 16 sample positions, located at the same distance from the center of rotation. We placed two substrates, namely, Suprasil substrate of 6.35 mm thickness and Glass B260 substrate of 1 mm thickness, exactly at the same distance from the rotation center of the turntable. At these positions, two corresponding samples denoted as QWM-2-Suprasil and QWM-2-Glass were produced. Uniformity between different positions was better than 0.2% of layer thickness. Magnetron sputtering is known as a process with a stable deposition rate and very dense layers (see, for example, [20,21]). In this situation, stability, homogeneity, and amorphous structure of produced films are provided.

Layer thicknesses were controlled using well-calibrated time monitoring [22,23]. The estimated level of thickness errors did not exceed 1% [19,20,24]. During the deposition of QWM-2-Suprasil and QWM-2-Glass samples, intentional relative errors equal to −7% and 7% were imposed on the third and twelfth layers, respectively. These errors were several times higher than the estimated level of errors associated with the monitoring procedure, and we expected that the reverse engineering algorithm was to be able to detect these intentional thickness errors.

By the analogy, in the fourth deposition run, we deposited two samples QWM-4-Suprasil and QWM-4-Glass with the intentional relative errors of 7%, −7%, −5%, and 5% made in thicknesses of the third, eighth, fourteenth, and fifteenth layers.

The HELIOS plant was also equipped with a BBM system [25]. In the course of the deposition, the BBM device worked in a passive mode for data acquisition only: broadband transmittance scans were recorded after deposition of each layer. The test samples QWM-2-Glass and QWM-4-Glass were placed on the position where the BBM monitoring system performed measurements. As a result, we had multiscan transmittance data related to the samples QWM-2-Glass and QWM-4-Glass. Transmittance data were taken in the spectral range from 400 to 950 nm, and the number of spectral points was 1239.

After the deposition, transmittance data of the QWM-2-Suprasil and QWM-4-Suprasil samples were taken at normal incidence in the spectral range from 330 to 1100 nm using Perkin Elmer Lambda 900 spectrophotometer. The number of spectral points was 771.

Then, for the single layer samples and the test samples QWM-2-Suprasil and QWM-4-Suprasil, ellipsometric measurements were performed using the M–2000UITM Spectroscopic Ellipsometer (J.A. Woollam Co., Inc.). For QWM-2-Suprasil and QWM-4-Suprasil samples, ellipsometric angles Ψ and Δ for AOI = 65° were measured in the spectral range from 245 to 1700 nm. For Ta_2O_5 and SiO_2 samples, ellipsometric angles Ψ and Δ were taken for AOI = 70° and AOI = 55.5°, respectively. The spectral range was from 245 to 1700 nm.

3. Reverse Engineering of Deposited Coatings

A. Refractive Indices of Layer Materials

Knowing refractive indices of layers with a high accuracy is important for successful reverse engineering of multilayer coatings [9,16,26]. For this reason, we started our study with specification of refractive indices used for calculations of theoretical characteristics and verification of consistency of films refractive indices obtained from different experimental data sets.

For calculating theoretical characteristics of test samples, we used so-called *nominal refractive indices* of Ta_2O_5 and SiO_2. These refractive indices were specified by the Cauchy formula:

$$n(\lambda) = A_0 + A_1\left(\frac{\lambda_0}{\lambda}\right)^2 + A_2\left(\frac{\lambda_0}{\lambda}\right)^4, \qquad (1)$$

where $A_0 = 2.06572$, $A_1 = 0.016830$, and $A_2 = 0.001686$ for Ta_2O_5 and $A_0 = 1.46529$, $A_1 = 0$, and $A_2 = 0.0004708$ for SiO_2; if wavelength λ in this formula is expressed in nanometers, then $\lambda_0 = 1000$ nm. Dispersion data of Suprasil substrate were taken from Heraeus Quartzglas Catalog [27]. Refractive index of Glass B260 substrate was described by the Cauchy formula with $A_0 = 1.500859$, $A_1 = 3.26477 \cdot 10^{-3}$, and $A_2 = 5.0404 \cdot 10^{-4}$; these coefficients were preliminary determined by fitting transmittance measurement data.

The nominal refractive indices were obtained on the basis of multiple characterization attempts of single layer and multilayer samples in the course of careful time-calibration of the HELIOS plant. These indices had typically been used in the course of the deposition of complicated dispersive mirrors containing dozens of layers. The indices therefore are known quite reliably, since dispersive mirrors are very sensitive to refractive index variations [20,22–24]. Nominal refractive indices are shown in Fig. 1 by solid black curves. Dashed gray curves in the same figure show refractive indices of Ta_2O_5 and SiO_2 obtained in [28] from measured transmittance data.

In Fig. 1, solid gray curves represent refractive indices of Ta_2O_5 and SiO_2 determined in the course of

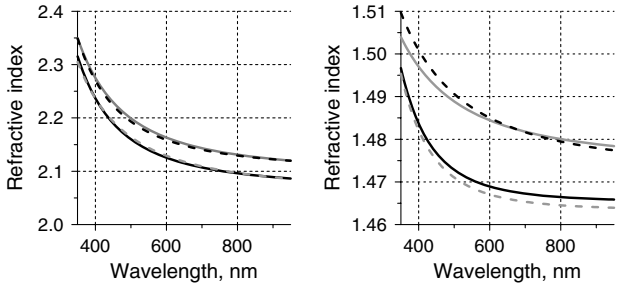

Fig. 1. Refractive indices of Ta_2O_5 films (left side) and SiO_2 films (right side): nominal indices (solid black curve), indices obtained in [28] (dashed gray curve), indices determined in [9] (solid gray curve), and indices obtained from ellipsometric measurement data (dashed black curve).

the characterization process based on multiangle spectral photometric data related to single layer samples [9]. Geometrical thicknesses of Ta_2O_5 and SiO_2 films were obtained equal to 292.3 and 401.4 nm, respectively.

In Fig. 1, dashed black curves present refractive index wavelength dependencies obtained as a result of a characterization process utilizing spectral ellipsometric data. Geometrical thicknesses of Ta_2O_5 and SiO_2 were found equal to 293.4 and 405.0 nm, respectively.

In Fig. 1, one can observe that *determined refractive indices* marked by solid gray curves and dashed black curves are consistent, although they were found from measurement data sets taken at completely different devices. There is also a good correspondence between determined geometrical thicknesses of the considered films: deviations between thickness values are 0.4% and 0.9% for Ta_2O_5 and SiO_2 films, respectively.

At the same time, it is seen from Fig. 1 that the determined refractive indices are shifted upwards in comparison with nominal refractive indices. Dispersion behavior of determined and nominal refractive indices is very similar. Determined refractive indices deviate from the nominal ones for 0.035 in the case of Ta_2O_5 films and for 0.02 in the case of SiO_2 films, which corresponds to 1.6% and 1.4% of the nominal refractive index values. These deviations can be explained by the fact that the nominal indices were obtained from experimental data related to coatings deposited on B260 Glass substrates of 1 mm thickness, while the determined refractive indices were obtained from data related to single layers on Suprasil substrates of 6.35 mm thickness. The difference in refractive indices may be connected with different microscopic structures of thin films deposited on different substrates and differences of optical properties of single films and films in a multilayer coating [29,30]. The difference can be explained also by the differences in measurements. They are more complicated in the case of thicker substrates, since both the main transmittance beam and at least the first double internal reflection (in transmission) or main beam and first reflection from the back face (in reflection) needed to be unobstructed and included in the measurements [9] and in the corresponding characterization model.

Comparison of Ta_2O_5 and SiO_2 refractive index wavelength dependencies convinced us that refractive indices of layers should be fitted in the course of the reverse engineering process. It is possible that refractive indices of films in a multilayer stack are slightly different from the refractive indices of single thin films used for optical characterization, since single films are several times thicker than typical thicknesses of layers forming a multilayer stack (see, for example, [31]). In our case, thicknesses of Ta_2O_5 and SiO_2 layers in the single layer samples were about four times more than thicknesses of corresponding layers in test samples. For this reason, we started our reverse engineering procedure by accounting for possible offsets of layer refractive indices from nominal ones. In this case, only two parameters have to be determined. This raises the stability of the the reverse engineering procedure, since attempts to simultaneously determine offsets of refractive indices and errors in layer thicknesses lead to unstable physically meaningless results.

B. Reverse Engineering Results Obtained on the Basis of Multiscan Measurements

We performed reverse engineering on the basis of analysis of transmittance scans taken for a set of wavelengths denoted as $\{\lambda_j\}$, $j = 1, \ldots, L$, where L is the number of wavelength points. Denote $\hat{T}^{(i)}(\lambda_j)$ as the transmittance scan acquired after terminating deposition of the ith layer. Denote as $T(d_1, \ldots, d_i; n_H(\lambda_j), n_L(\lambda_j); \lambda_j)$ the model transmittance data for the first i deposited coating layers. In our reverse engineering procedure, we utilized all transmittance scans simultaneously and used the triangular algorithm for layer parameters determination [16].

In order to estimate a closeness between theoretical and experimental data, we introduced the *multiscan discrepancy function*:

$$\mathrm{MDF}^2 = \frac{1}{NL}\sum_{i=1}^{N}\sum_{j=1}^{L}[T(\mathbf{X};\lambda_j) - \hat{T}^{(i)}(\lambda_j)]^2, \qquad (2)$$

where $N = 15$ is the number of layers in the coating and $\mathbf{X}$ is the vector of parameters describing our coating. The MDF values [Eq. (2)] were 3.06 for QWM-2-Glass sample and 4.13 for QWM-4-Glass sample.

Our reverse engineering procedure consisted of two steps. At the first step, we introduced a model, in which the theoretical transmittance $T(\mathbf{X};\lambda)$ in Eq. (2) depends on two unknown parameters, namely refractive index offsets h_H and h_L:

$$T(\mathbf{X},\lambda) = T(d_1, \ldots, d_i; n_H(\lambda) + h_H, n_L(\lambda) + h_L; \lambda). \quad (3)$$

This model reduced the multiscan discrepancy function Eq. (2) to the function of two parameters

$$\mathrm{MDF}^2 = \mathrm{MDF}^2(h_H, h_L). \qquad (4)$$

After minimization of the MDF function with respect to these two parameters h_H and h_L, MDF values became 2.6 for QWM-2-Glass and 2.8 for QWM-4-Glass samples. *Corrected refractive indices* $\tilde{n}_H = n_H + h_H$ and $\tilde{n}_L = n_L + h_L$ corresponding to QWM-2-Glass and QWM-4-Glass samples are shown in Fig. 2 by gray curve (2) and black curve (3), respectively.

At the second step of our reverse engineering procedure, we introduced a model of relative errors in layer thicknesses:

$$T(\mathbf{X};\lambda) = T((1+\delta_1)d_1, \ldots, (1+\delta_i)d_i; \tilde{n}_H(\lambda), \tilde{n}_L(\lambda); \lambda). \qquad (5)$$

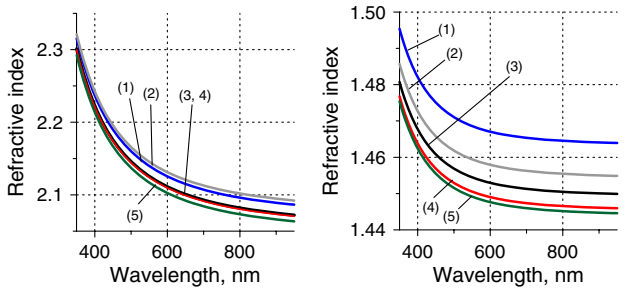

Fig. 2. (Color online) Refractive indices of Ta_2O_5 films (left panel) and SiO_2 films (right panel): nominal indices (1—solid blue curve), indices obtained from multiscan measurements related to QWM-2-Glass sample (2—gray curve) and to QWM-4-Glass sample (3—black curve), indices determined from Perkin Elmer measurements related to QWM-2-Suprasil sample (4—red curve) and to QWM-4-Suprasil sample (5—green curve). Curves 3 and 4 are almost undistinguishable at the left panel.

With this model, the multiscan discrepancy function was reduced to the function of $N = 15$ parameters

$$\mathrm{MDF}^2 = \mathrm{MDF}^2(\delta_1, \ldots, \delta_N), \tag{6}$$

and the minimization of MDF function (6) with respect to $\delta_1, \ldots, \delta_N$ provided final discrepancies 0.87 and 0.5 for QWM-2-Glass and QWM-4-Glass samples, respectively.

Determined relative errors are shown in Fig. 3 by black bars. The intended errors are shown in this figure by gray bars. In Fig. 3, one can observe that the intended errors were detected reliably; the difference between determined relative errors does not exceed the estimated accuracy of thickness monitoring. Errors in layers without imposed thickness errors do not exceed 2%. These errors can be caused by two reasons. The first one is some inaccuracy of the time monitoring. The second one is the instability of the reverse engineering procedure as well as the effect of errors in measurement data. It was demonstrated in [16] that errors of 1% magnitude can be caused by random noise and systematic offsets of measurement transmittance scans.

In this subsection, we have shown that reverse engineering results obtained on the basis of analysis of multiscan measurements can be considered as reliable ones.

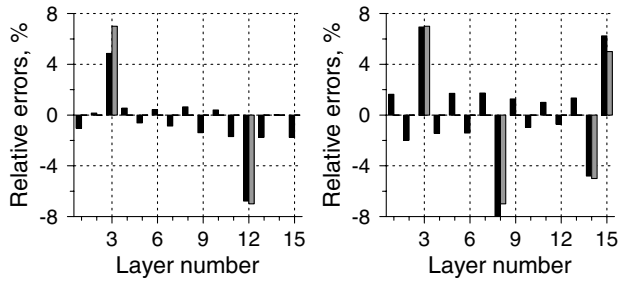

Fig. 3. Black bars present relative errors in layer thicknesses of QWM-2-Glass sample (left panel) and QWM-4-Glass sample (right panel) determined on the basis of multiscan transmittance data. Gray bars show errors imposed on layer thicknesses.

C. Reverse Engineering Results Obtained Using Offline Transmittance Data Array

At our disposal, we had normal incidence transmittance data $\hat{T}(\lambda_j)$ taken by a Perkin Elmer spectrophotometer in the spectral range from 330 to 950 nm. We performed two reverse engineering attempts. First, we performed reverse engineering on the basis of transmittance data taken in the visible spectral range. Data taken in the range from 380–400 nm to 800–1000 nm are frequently used in the reverse engineering procedure [15,32].

In order to estimate a closeness between theoretical and experimental data, we introduced a *discrepancy function*:

$$\mathrm{DF}^2 = \frac{1}{L}\sum_{j=1}^{L}[T(\mathbf{X};\lambda_j) - \hat{T}(\lambda_j)]^2. \tag{7}$$

The initial DF values were 7.60 for the QWM-2-Suprasil sample and 4.45 for the QWM-4-Suprasil sample. The number of spectral points L was 551.

For the reverse engineering, we applied a sequence of models similar to the previous subsection. At the first step, we introduced a model, in which the theoretical transmittance $T(\mathbf{X}, \lambda)$ in Eq. (7) depends on two unknown refractive index offsets h_H and h_L:

$$T(\mathbf{X}, \lambda) = T(d_1, \ldots, d_N; n_H(\lambda) + h_H, n_L(\lambda) + h_L; \lambda). \tag{8}$$

This model reduced the discrepancy function Eq. (7) to the function of two parameters

$$\mathrm{DF}^2 = \mathrm{DF}^2(h_H, h_L), \tag{9}$$

and after minimization DF values became 3.14 and 4.28 for QWM-2-Suprasil and QWM-4-Suprasil samples, respectively.

At the second step of our reverse engineering procedure, we introduced a model of relative errors in layer thicknesses:

$$T(\mathbf{X};\lambda) = T((1+\delta_1)d_1, \ldots, (1+\delta_N) \times d_N; \tilde{n}_H(\lambda), \tilde{n}_L(\lambda); \lambda). \tag{10}$$

With this model, the discrepancy function was reduced to the function of $N = 15$ parameters

$$\mathrm{DF}^2 = \mathrm{DF}^2(\delta_1, \ldots, \delta_N), \tag{11}$$

and minimization of this function allowed us to obtain relative errors in layer thicknesses $\delta_1, \ldots, \delta_N$. The achieved final discrepancies were equal to 0.67 and 0.65 for QWM-2-Suprasil and QWM-4-Suprasil samples, respectively. Estimated $\delta_1, \ldots, \delta_N$ values are presented in Fig. 4. In this figure one can see that in the case of the QWM-2-Suprasil sample, only the error in twelfth layer was detected with a sufficient accuracy. The error in the third layer was reproduced with an accuracy of 2%. The obtained

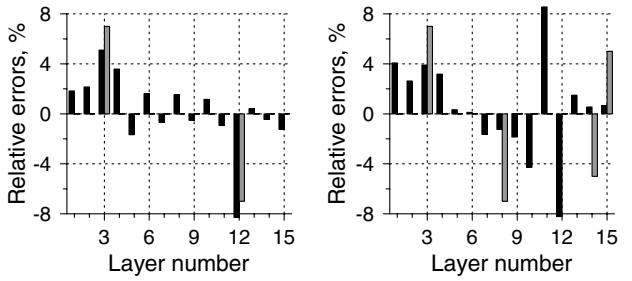

Fig. 4. Black bars present relative errors in layer thicknesses of QWM-2-Suprasil sample (left panel) and QWM-4-Suprasil sample (right panel) determined on the basis of transmittance data taken by the Perkin Elmer spectrophotometer in the spectral range from 400 to 950 nm. Gray bars show errors imposed on layer thicknesses.

error of about 4% in the fourth layer is incorrect. In the case of the QWM-4-Suprasil sample, the estimated relative errors do not correspond to the intended errors.

At the second reverse engineering attempt, we utilized the transmittance data from the range 330–950 nm; the number of spectral points was $L = 621$. This spectral range was wider than the range used in the first reverse engineering attempt. For this attempt, we used the same reverse engineering procedure as for the first attempt.

In this case, the initial discrepancies were 4.47 and 4.37; intermediate DF values [Eq. (10)] 4.3 and 4.2 were obtained for QWM-2-Suprasil and QWM-4-Suprasil samples, respectively. Corrected refractive indices are shown in Fig. 2 by red curve (4) and green curve (5). At the second step of the reverse engineering procedure, final discrepancy values equal to 0.57 and 0.66 were achieved for QWM-2-Suprasil and QWM-4-Suprasil samples, respectively. Determined relative errors $\delta_1, \ldots, \delta_N$ are presented in Fig. 5 by black bars. In the case of the QWM-2-Suprasil sample, the intended errors in the third and twelfth layers were found correctly. The levels of errors in other layers do not exceed estimated accuracy of the time monitoring procedure. In the case of the QWM-4-Suprasil sample, the imposed errors were detected with good accuracy. Some other errors reach 3%,

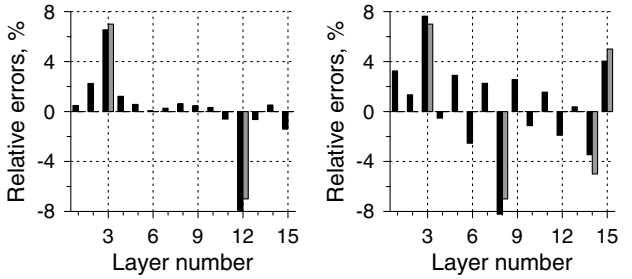

Fig. 5. Black bars present relative errors in layer thicknesses of QWM-2-Suprasil sample (left panel) and QWM-4-Suprasil sample (right panel) determined on the basis of transmittance data taken by the Perkin Elmer spectrophotometer in the spectral range from 330 to 950 nm. Gray bars show errors imposed on layer thicknesses.

which is a bit higher than estimated accuracy of thickness control with time monitoring. This can be considered as an effect of instability of the reverse engineering procedure.

An additional comment should be made here. The final discrepancies achieved in the course of two reverse engineering attempts were close: 0.67 and 0.57 for the QWM-2-Suprasil sample, and 0.57 and 0.66 for the QWM-4-Suprasil sample. At the same time, reverse engineering results were absolutely different. Moreover, in the first attempt, these results were wrong, and in the second attempt, the results were correct. Therefore a small value of the discrepancy (good fitting) cannot be considered as an indication of reliable reverse engineering results. Utilization of additional *a priori* information and careful checks of results consistency should always be performed.

Reverse engineering results obtained above convinced us that the measurement spectral range played an important role in optical parameters determination in cases when the offline spectral photometric data array related to produced samples was used. For our test samples, the spectral range from 330 to 400 nm was critical because transmittance spectral dependencies have informative oscillating features in this range. In the left panel of Fig. 6, we present fitting of measurement data in the spectral range from 330 to 950 nm by model transmittance calculated on the basis of layer thicknesses found for the QWM-4-Suprasil sample in the course of the first reverse engineering attempt (experimental data were taken from the range 400–950 nm). We observe that fitting in the short wavelength spectral range 330–400 nm is quite bad; oscillating features are not fitted by model curve. In the right panel of Fig. 6, we demonstrate the excellent fitting of the same measurement data by model transmittance calculated on the basis of layer thicknesses found for the QWM-4-Suprasil sample in the course of the second reverse engineering attempt (experimental data from the range 330–950 nm were explored).

D. Analysis of Spectral Ellipsometric Data

In this subsection, we investigate whether reliable reverse engineering results can be obtained on the basis of analysis of spectral ellipsometric data. In

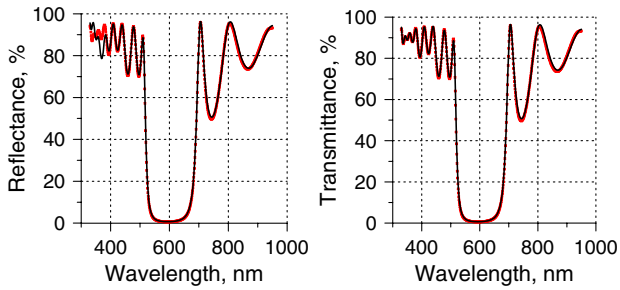

Fig. 6. (Color online) Fitting of experimental data (red crosses) by model transmittance (black curve) when reverse engineering was performed using experimental data in the range 400–950 nm (left panel) and in the range 330–950 nm (right panel).

our research, we processed the ellipsometric data from the spectral range 330–1100 nm, where material absorption may be neglected.

In order to estimate the closeness between measured ellipsometric angles $\Psi(\lambda_j)$ and $\Delta(\lambda_j)$ and theoretical ellipsometric angles $\Psi(\mathbf{X};\lambda_j)$ and $\Delta(\mathbf{X};\lambda_j)$, we calculated discrepancies using the following formula:

$$\mathrm{DF}^2 = \frac{1}{2L}\left\{\sum_{j=1}^{L}\left[\frac{\Psi(\mathbf{X};\lambda_j)-\hat{\Psi}(\lambda_j)}{\Delta\Psi_j}\right]^2 + \sum_{j=1}^{L}\left[\frac{\Delta(\mathbf{X};\lambda_j)-\hat{\Delta}(\lambda_j)}{\Delta\Delta_j}\right]^2\right\}, \quad (12)$$

where $\Delta\Psi_j$ and $\Delta\Delta_j$ are measurement errors in Ψ and Δ data delivered by the Woollam ellipsometer.

Initial discrepancies were equal to 226.0 and 191.9 for QWM-2-Suprasil and QWM-4-Suprasil samples, respectively. Note that significantly higher values of discrepancies in the case of ellipsometry are caused by measurement errors $\Delta\Psi_j$ varying in the range [0.008, 0.2] and $\Delta\Delta_j$ varying in the range [0.016, 8.6] in Eq. (12). One should not compare these values with spectrophotometric case discrepancies; only relative decrease of the discrepancy value for the same data set is important.

First, we performed reverse engineering of the test coatings using OptiRE software [12]. The sequence of models was selected analogous to the previous two subsections.

At the first step, we introduced the model of refractive indices offsets:

$$\Psi(\mathbf{X},\lambda) = \Psi(d_1,\ldots,d_N;n_H(\lambda)+h_H,n_L(\lambda)+h_L;\lambda),$$
$$\Delta(\mathbf{X},\lambda) = \Delta(d_1,\ldots,d_N;n_H(\lambda)+h_H,n_L(\lambda)+h_L;\lambda). \quad (13)$$

This model reduced the discrepancy function Eq. (12) to the function of two parameters DF^2 similar to Eq. (9). After indices correction, DF values were 205.1 and 177.2 for QWM-2-Suprasil and QWM-4-Suprasil test samples, respectively.

At the second step of the reverse engineering procedure, we introduced a model of relative errors in layer thicknesses:

$$\Psi(\mathbf{X};\lambda) = \Psi((1+\delta_1)d_1,\ldots,(1+\delta_N) \times d_N;\tilde{n}_H(\lambda),\tilde{n}_L(\lambda);\lambda),$$
$$\Delta(\mathbf{X};\lambda) = \Delta((1+\delta_1)d_1,\ldots,(1+\delta_N) \times d_N;\tilde{n}_H(\lambda),\tilde{n}_H(\lambda);\lambda). \quad (14)$$

With this model, the discrepancy function was reduced to the function of $N = 15$ parameters similar to Eq. (11), and minimization of this function allowed us to obtain final discrepancies equal to 62.4 and 58.5 for QWM-2-Suprasil and QWM-4-Suprasil samples, respectively. The estimated relative errors are shown in Fig. 7 by black bars. It is evident that the estimated errors have nothing in common with intended errors. This means that we obtained wrong reverse engineering results. We can suppose therefore that ellipsometric data related to a produced multilayer sample cannot be considered as a basis for reliable engineering of this sample, at least in the frame of the selected models. It is likely that elaboration of more complicated specialized models can improve the situation with ellipsometric data processing, but this goes outside the scope of the current work.

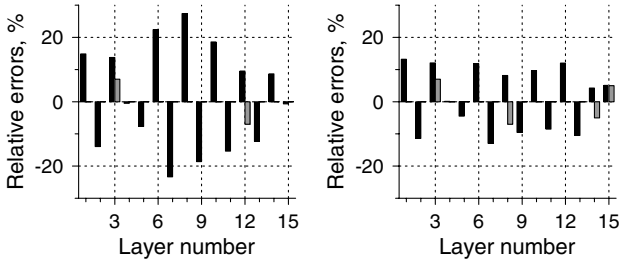

Fig. 7. Black bars present relative errors in layer thicknesses of the QWM-2-Suprasil sample (left panel) and the QWM-4-Suprasil sample (right panel) determined on the basis of ellipsometric measurements with the help of OptiRE software. Gray bars show errors imposed on layer thicknesses.

There is another issue related to the reverse engineering procedure. One may ask whether a sequence of reverse engineering steps or numerical algorithm of discrepancy function minimization affect the results. In order to answer this question, we performed reverse engineering of the test samples with the help of Woollam software [10] using an approach similar to that described above.

Relative errors in layer thicknesses are shown in Fig. 8 by black bars. As in the case of reverse engineering with OptiRE software, one can observe disagreement between intended and estimated errors. This inconsistency indicates that the reverse engineering results are unreliable.

On the basis of the analysis provided in this subsection, we demonstrated that in the cases of our test samples, the reliable reverse engineering results cannot be found from ellipsometric data. We do not state here that ellipsometric data cannot be used for reverse engineering at all. Probably, these data provide reliable results in the cases when the

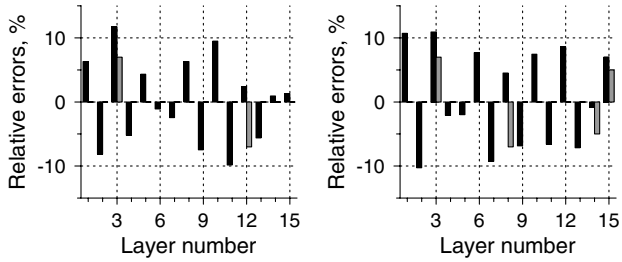

Fig. 8. Black bars present relative errors in layer thicknesses of the QWM-2-Suprasil sample (left panel) and the QWM-4-Suprasil sample (right panel) determined on the basis of ellipsometric measurements with the help of Woollam software. Gray bars show errors imposed on layer thicknesses.

number of coating layers is relatively small or if these data are used in the combination with photometric data. This issue, however, requires a distinct comprehensive study.

4. Conclusions

We performed reverse engineering of test samples with known errors in layer thicknesses. As the basis for the reverse engineering, we used different measurement data sets, namely, multiscan measurements taken *in situ* by the BBM spectrophotometer, single transmittance spectra measured using the Perkin Elmer spectrophotometer, and ellipsometric angles. In all reverse engineering attempts, we used the same procedure: indices correction and successive estimation of errors in layer thicknesses. We demonstrated the following:

- Multiscan transmittance spectra can be used for reliable reverse engineering of multilayer optical coatings.
- Reliability of the reverse engineering results obtained from single measurement data array is strongly dependent on the spectral range in which the data are used. Measured spectral characteristic should contain informative features in this range.
- Reliability of the reverse engineering results on the basis of analysis of ellipsometric data is problematic. In our study, we demonstrated the situation when ellipsometric measurements cannot be used for reliable reverse engineering.

In our study, we demonstrated that there are data sets that can be definitely used for reliable reverse engineering and there are data sets that can provide reliable and unreliable results. Future work on this topic may include a comprehensive experimental and numerical study aimed at revealing the dependence of reverse engineering results on the number of coating layers.

Funding by the German Research Foundation (DFG) within the Clusters of Excellence "Munich Centre for Advanced Photonics" (MAP) (htpp://www.munich-photonics.de) and "Centre of Quantum Engineering and Space Time Research" (QUEST), as well as the Russian Fund of Basic Research, project 10-07-00480-a, is gratefully acknowledged.

References

1. J. Oliver, A. Tikhonravov, M. Trubetskov, I. Kochikov, and D. Smith, "Real-time characterization and optimization of e-beam evaporated optical coatings," in *Optical Interference Coatings*, Technical Digest (Optical Society of America, 2001), paper ME8.
2. S. Wilbrandt, O. Stenzel, N. Kaiser, M. K. Trubetskov, and A. V. Tikhonravov, "In situ optical characterization and reengineering of interference coatings," Appl. Opt. **47**, C49–C54 (2008).
3. D. Ristau, H. Ehlers, S. Schlichting, and M. Lappschies, "State of art in deterministic production of optical thin films," Proc. SPIE **7101**, 71010C (2008).
4. T. V. Amotchkina, M. K. Trubetskov, V. Pervak, and A. V. Tikhonravov, "Design, production and reverse engineering of two-octave antireflection coatings," Appl. Opt. **50**, 6468–6475 (2011).
5. A. N. Tikhonov and V. Y. Arsenin, *Solutions of Ill-Posed Problems* (Wiley, 1977).
6. V. Janicki, J. Sancho-Parramon, O. Stenzel, M. Lappschies, B. Goertz, C. Rickers, C. Polenzky, and U. Richter, "Optical characterization of hybrid antireflective coatings using spectrophotometric and ellipsometric measurements," Appl. Opt. **46**, 6084–6091 (2007).
7. R. Andrade, E. G. Birgin, I. Chambouleyron, J. M. Martinez, and S. D. Ventura, "Estimation of the thickness and the optical parameters of several stacked thin films using optimization," Appl. Opt. **47**, 5208–5220 (2008).
8. A. Tikhonravov, M. Trubetskov, V. Pervak, F. Krausz, and A. Apolonski, "Design, fabrication and reverse engineering of broad band chirped mirrors," in *Optical Interference Coatings*, Technical Digest (CD) (Optical Society of America, 2007), paper WB4.
9. A. V. Tikhonravov, T. V. Amotchkina, M. K. Trubetskov, R. Francis, V. Janicki, J. Sancho-Parramon, H. Zorc, and V. Pervak, "Optical characterization and reverse engineering based on multiangle spectroscopy," Appl. Opt. **51**, 245–254 (2012).
10. J. Woollam, *WVASE Manual. Guide to Using WVASE32* (WexTech Systems Inc., 1996).
11. H. Fujuwara, *Specroscopic Ellipsometry. Principles and Applications* (Wiley, 2007).
12. A. V. Tikhonravov and M. K. Trubetskov, OptiLayer thin film software, http://www.optilayer.com.
13. A. V. Tikhonravov, M. K. Trubetskov, J. Hrdina, and J. Sobota, "Characterization of quasi-rugate filters using ellipsometric measurements," Thin Solid Films **277**, 83–89 (1996).
14. T. V. Amotchkina, V. Janicki, J. Sancho-Parramon, A. V. Tikhonravov, M. K. Trubetskov, and H. Zorc, "General approach to reliable characterization of thin metal films," Appl. Opt. **50**, 1453–1464 (2011).
15. A. V. Tikhonravov and M. K. Trubetskov, "On-line characterization and reoptimization of optical coatings," Proc. SPIE **5250**, 406–413 (2004).
16. T. V. Amotchkina, M. K. Trubetskov, V. Pervak, S. Schlichting, H. Ehlers, D. Ristau, and A. V. Tikhonravov, "Comparison of algorithms used for optical characterization of multilayer optical coatings," Appl. Opt. **50**, 3389–3395 (2011).
17. S. Wilbrandt, O. Stenzel, and N. Kaiser, "All-optical in-situ analysis of piad deposition processes," Proc. SPIE **7101**, 71010D (2008).
18. B. Badoil, F. Lemarchand, M. Cathelinaud, and M. Lequime, "Interest of broadband optical monitoring for thin-film filter manufacturing," Appl. Opt. **46**, 4294–4303 (2007).
19. V. Pervak, A. V. Tikhonravov, M. K. Trubetskov, J. Pistner, F. Krausz, and A. Apolonski, "Band filters: 2-material technology versus rugate," Appl. Opt. **46**, 1190–1193 (2007).
20. V. Pervak, M. K. Trubetskov, and A. V. Tikhonravov, "Robust synthesis of dispersive mirrors," Opt. Express **19**, 2371–2380 (2011).
21. V. Pervak, C. Teisset, A. Sugita, S. Naumov, F. Krausz, and A. Apolonski, "High-dispersive mirrors for femtosecond lasers," Opt. Express **16**, 10220–10233 (2008).
22. V. Pervak, A. V. Tikhonravov, M. K. Trubetskov, S. Naumov, F. Krausz, and A. Apolonski, "1.5-octave chirped mirror for pulse compression down to sub-3 fs," Appl. Phys. B **87**, 5–12 (2007).
23. V. Pervak, I. Ahmad, J. Fülop, M. K. Trubetskov, and A. V. Tikhonravov, "Comparison of dispersive mirrors based on the time-domain and conventional approaches, for sub-5 fs pulses." Opt. Express **17**, 2207–2217 (2009).
24. V. Pervak, "Recent developments and new ideas in the field of dispersive multilayer optics," Appl. Opt. **50**, C55–C61 (2011).
25. D. Ristau, H. Ehlers, T. Gross, and M. Lappschies, "Optical broadband monitoring of conventional and ion processes," Appl. Opt. **45**, 1495–1501 (2006).
26. K. Friedrich, S. Wilbrandt, O. Stenzel, N. Kaiser, and K. Hoffmann, "Computational manufacturing of optical interference coatings: method, simulation results, and comparison with experiment," Appl. Opt. **49**, 3150–3162 (2010).
27. Quartz Glass for Optics: Data and Properties, http://heraeus-quarzglas.com.

28. A. V. Tikhonravov, M. K. Trubetskov, T. V. Amotchkina, G. DeBell, V. Pervak, A. K. Sytchkova, M. L. Grilli, and D. Ristau, "Optical parameters of oxide films typically used in optical coating production," Appl. Opt. **50**, C75–C85 (2011).
29. D. Ristau, S. Günster, S. Bosch, A. Duparré, E. Masetti, J. Ferré-Borrull, G. Kiriakidis, F. Peiró, E. Quesnel, and A. Tikhonravov, "Ultraviolet optical and microstructural properties of MgF_2 and LaF_3 coatings deposited by ion-beam sputtering and boat and electron-beam evaporation," Appl. Opt. **41**, 3196–3204 (2002).
30. M. Modreanu, J. Sancho-Parramon, D. O'Connell, J. Justice, O. Durand, and B. Servet, "Solid phase crystallisation of hfo2 thin films," Mater. Sci. Eng., B **118**, 127–131 (2005).
31. A. Tikhonravov, M. Trubetskov, T. Amotchkina, A. Tikhonravov, D. Ristau, and S. Günster, "Reliable determination of wavelength dependence of thin film refractive index," Proc. SPIE **5188**, 331–342 (2003).
32. A. V. Tikhonravov, M. K. Trubetskov, M. A. Kokarev, and S. Thony, "Reverse engineering of fabricated coatings using off-line and on-line photometric data," in *Optical Interference Coatings*, Technical Digest (CD) (Optical Society of America, 2007), paper WA3.